Neuron
Review

Inhibition, Spike Threshold, and Stimulus Selectivity in Primary Visual Cortex

Nicholas J. Priebe[1] and David Ferster[2,*]
[1]Section of Neurobiology, The University of Texas at Austin, 1 University Station C0920, Austin, TX 78712, USA
[2]Department of Neurobiology and Physiology, Northwestern University, 2205 Tech Drive, Evanston, IL 60208, USA
*Correspondence: ferster@northwestern.edu
DOI 10.1016/j.neuron.2008.02.005

Ever since Hubel and Wiesel described orientation selectivity in the visual cortex, the question of how precise selectivity emerges has been marked by considerable debate. There are essentially two views of how selectivity arises. Feed-forward models rely entirely on the organization of thalamocortical inputs. Feedback models rely on lateral inhibition to refine selectivity relative to a weak bias provided by thalamocortical inputs. The debate is driven by two divergent lines of evidence. On the one hand, many response properties appear to require lateral inhibition, including precise orientation and direction selectivity and crossorientation suppression. On the other hand, intracellular recordings have failed to find consistent evidence for lateral inhibition. Here we demonstrate a resolution to this paradox. Feed-forward models incorporating the intrinsic nonlinear properties of cortical neurons and feed-forward circuits (i.e., spike threshold, contrast saturation, and spike-rate rectification) can account for properties that have previously appeared to require lateral inhibition.

Since Hartline described inhibition between adjacent photoreceptors in the *limulus* retina (Hartline, 1949), the principle of lateral inhibition has become deeply embedded in neuroscience. In Hartline's original experiments, lateral inhibition operated purely in the spatial domain, heightening the difference between adjacent photoreceptors' responses to a spatially localized stimulus. The modern concept of lateral inhibition has expanded to incorporate distance along almost any axis in sensory space, in virtually every sensory modality. Lateral inhibition is thought to occur between whiskers in the somatosensory system (Moore and Nelson, 1998; Zhu and Connors, 1999), between odors in the olfactory system (Wilson and Mainen, 2006), between sounds of different frequency (Brosch and Schreiner, 1997; Calford and Semple, 1995), between different phonemes (Crutch and Warrington, 2001; Mirman et al., 2005), and between different tastes in the gustatory system (Vandenbeuch et al., 2004). An underlying assumption in each case is that the excitatory afferents from the earlier stages of processing provide a weak bias toward a preferred stimulus and establish only a rough outline of a cell's tuning. Lateral inhibition then sharpens sensory tuning to its final state by vetoing any residual excitation evoked by nonpreferred stimuli. In this way, lateral inhibition could provide considerable computational power to neuronal circuits.

In the primary visual cortex (V1), lateral inhibition has been proposed to refine neuronal selectivity in a number of domains, sharpening orientation and direction tuning, making tuning independent of stimulus strength, and generating suppressive interactions between different stimuli (Crook et al., 1998; Eysel et al., 1990; Sompolinsky and Shapley, 1997; Worgotter and Eysel, 1991). And yet, inhibition measured in intracellular recordings from primary sensory areas often lacks the necessary properties to support lateral inhibition: inhibitory inputs are most often tuned to the same stimuli as the excitatory inputs, and inhibition evoked by nonpreferred stimuli is generally weak (Anderson et al., 2000a; Tan et al., 2004; Wehr and Zador, 2003). In addition, inactivation of the cortical circuit (including both excitatory and inhibitory components) does not degrade the selectivity derived from the remaining feed-forward synaptic inputs (Chung and Ferster, 1998; Ferster et al., 1996).

For orientation selectivity in particular, the contradiction between these two lines of evidence—the apparent need for lateral inhibition to explain response properties, and the apparent lack of lateral inhibition observed in many experiments—has driven considerable controversy. Here, we discuss these two divergent views and outline a possible resolution. We find that a simple feed-forward model—without the inclusion of lateral inhibition—can replicate the receptive field properties of cortical neurons in considerable detail. That is, the complex aspects of cortical responses that have most often been attributed to lateral inhibition can be explained parsimoniously from simple, well-characterized, nonlinear features of the feed-forward excitatory pathways, such as spike threshold, contrast saturation, and spike rectification.

One goal of systems neuroscience lies in understanding the mechanisms underlying high-level processing, such as object recognition, language, and decision making. We are, however, just at the early stages of defining the computations that are performed in accomplishing these tasks, let alone understanding the circuitry that performs them. In contrast, the computations performed by V1—extracting orientation and direction of motion from the visual image, for example—are simple enough to define and measure with great precision and yet complex enough to be interesting, making the visual cortex an ideal area in which to study neural computation in detail. Because of the relative homogeneity of the cortical circuitry from area to area, most students of primary visual cortex subscribe to the view that what we learn about the principles of cortical processing there will apply to higher levels (Creutzfeldt, 1977). If this belief is correct, then the question of whether lateral inhibition is a critical

component of processing in primary visual cortex has implications throughout cortex.

Orientation Selectivity

When Hubel and Wiesel (1962) first described cortical orientation selectivity, they proposed an elegantly simple model for its origin that still serves as a central reference point. According to the model, simple cells in V1, the primary thalamo-recipient cells, become orientation selective by virtue of convergent input from thalamic neurons whose receptive fields are arranged in rows. A stimulus of the preferred orientation therefore activates all of the relay cells in a row simultaneously (Figure 1A), whereas the orthogonal (null) orientation activates only a few relay cells at a time. By virtue of the simple cell's spike threshold, only the large-amplitude response to the preferred stimulus evokes action potentials (Figure 1B).

There is compelling evidence that the spatial organization of the feed-forward input generates the ON-OFF spatial organization of simple cells' receptive fields and a consequent bias for orientation. (1) Simple cells are located in layers 4 and 6, the layers in which geniculate relay cell axons terminate (Hirsch and Martinez, 2006; Martinez et al., 2005). (2) The aggregate preferred orientation of the relay cells that innervate a cortical orientation column matches the preferred orientation of the cells in the column (Chapman et al., 1991). A similar match occurs in the connection between layer 4 to layer 2/3, where orientation selectivity emerges in the tree shrew (Mooser et al., 2004). (3) The majority of simple cells receive monosynaptic input from geniculate relay cells (Ferster et al., 1996; Ferster and Lindström, 1983). (4) Any relay cell that connects to a simple cell has the matching polarity (ON- or OFF-center) to the simple cell subfield with which its receptive field overlaps (Reid and Alonso, 1995; Jin et al., 2008; Tanaka, 1983).

While purely feed-forward models have been able to account for the foundation of cortical orientation tuning, up to now they have been largely unable to account for a number of critical features of simple cell behavior. These include (1) the sharpness of orientation tuning, which is far narrower than predicted by the spatial organization of the feed-forward input; (2) crossorientation suppression, in which a stimulus of the nonpreferred orientation suppresses the response to a stimulus of the preferred orientation; (3) contrast invariance of orientation tuning, in which simple cells fail to respond to nonpreferred stimuli of any strength (contrast), and the width of orientation tuning varies little with changes in the contrast; and (4) dynamics of orientation tuning, in which tuning width narrows over the time course of a response. These apparent failures of feed-forward models have long been considered to be classical cases in which lateral inhibition—in the form of crossorientation inhibition—is required to shape neuronal selectivity. We will examine each of these features in turn and show that each can, in fact, be accounted for by excitatory relay cell input to simple cells, without lateral inhibition.

Here, we focus almost exclusively on the visual cortex of the cat, where many of the relevant experiments have been performed. In the primate visual cortex, an additional set of orientation unselective cells in layer 4C is likely interposed between the thalamic relay cells and orientation selective simple cells (Hubel and Wiesel, 1968). Although they remain to be tested, many of the same arguments that we make here for the cat visual cortex might apply to the primate visual cortex.

The Sharpness of Orientation Tuning

If orientation tuning were derived solely from the spatial organization of relay cell input, an important prediction would follow: it should be possible, using a simple linear model, to derive the orientation tuning curve of any simple cell from a detailed map of its receptive field. In cells with short, wide subregions (Figure 2A, bottom), a bar stimulus can be rotated far away from the preferred orientation and still overlap with a large portion of the ON region, giving rise to broad orientation tuning. In contrast, long, narrow receptive field subregions (Figure 2A, top) should make a cell extremely sensitive to small changes in orientation and give rise to a narrow orientation tuning curve. While this general trend is often observed, the predicted quantitative relationship between receptive field maps and orientation tuning width is not. When based on the firing rate responses of neurons, the measured orientation tuning is up to three times narrower than linear predictions (Figure 2B) (Gardner et al., 1999; Jones and Palmer, 1987).

This mismatch has often been interpreted as evidence for lateral inhibition between neurons of different orientation preferences, also called crossorientation inhibition (Figure 2C, red curve). Such inhibition could suppress the effect of feed-forward excitation at nonpreferred orientations (green curve), thereby narrowing the tuning of the net changes in membrane potential (black curve). In the figure, inhibition peaks at orientations away from the preferred orientation. Lateral inhibition could also peak at the preferred orientation and be more broadly tuned than excitation or be largely untuned for orientation (Ben-Yishai et al., 1995; Hirsch et al., 2003; Somers et al., 1995; Sompolinsky et al., 1990; Sompolinsky and Shapley, 1997; Troyer et al., 2002). In either case, inhibition evoked by stimuli far from the preferred orientation would suppress the excitatory input and effectively narrow the orientation tuning of the spike output.

The most direct way to test for the presence of synaptic inhibition is through intracellular recording. Inhibition could reveal itself as a frank hyperpolarization. Simultaneous excitation and inhibition, however, might antagonize one another and generate no net change in membrane potential, making it necessary to measure changes in inhibitory conductance, either using voltage-clamp in vivo (Borg-Graham et al., 1998), or current-clamp with different levels of injected current (Anderson et al., 2000a; Douglas et al., 1991; Ferster, 1986; Hirsch et al., 1998; Martinez et al., 2002). In these latter studies, synaptic inhibition in layer 4 cells was tuned to the same orientation as synaptic excitation and firing rate responses. The preferred stimulus increases the conductance of a cell by 100% or more (Anderson et al., 2000a; Borg-Graham et al., 1998; Douglas et al., 1991; Ferster, 1986; Martinez et al., 2002). Null-oriented stimuli, by comparison, rarely increase the conductance of a neuron by more than 25%, and most often by far less (Anderson et al., 2000a; Priebe and Ferster, 2006), which may be too small to make a significant contribution to orientation selectivity.

A second method to determine whether intracortical inhibition shapes orientation tuning is to measure orientation tuning while inactivating inhibition. The removal of inhibition by extracellular

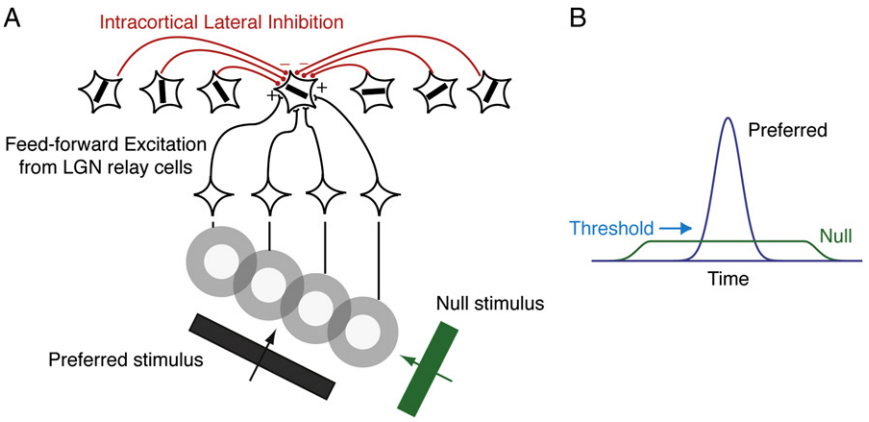

Figure 1. Models of Visual Cortex

(A) In the standard feed-forward model, cortical simple cells receive excitation from geniculate relay cells with their receptive fields aligned with the preferred orientation of the simple cells (black). In feedback or crossorientation inhibition models, simple cells, in addition, receive inhibition from inhibitory interneurons with different preferred orientations, or from interneurons that are untuned for orientation.

(B) The feed-forward input to the simple cell generates a short, high-amplitude depolarization in response to a stimulus of the preferred orientation (black) and a longer, low-amplitude depolarization in response to an orthogonally oriented stimulus (green). Only the former rises above threshold and triggers action potentials.

application of bicuculline does indeed alter receptive field structure (Sillito, 1975) and broaden orientation tuning (Sillito et al., 1980). There is some question, however, as to whether widespread inactivation of inhibition may render the cortical network unstable and thereby broaden the orientation tuning of intracortical excitation. To avoid this potential problem, inhibitory input was selectively inactivated in single cortical neurons by intracellular application of DIDS or picrotoxin (Nelson et al., 1994), with little effect on orientation tuning. As an alternative to pharmacological inactivation, intracortical inhibition and excitation were inactivated simultaneously by local cooling (Ferster et al., 1996) or electrical stimulation (Chung and Ferster, 1998). In both cases, the remaining synaptic inputs, which predominately arise from the thalamic feed-forward pathway, had similar orientation tuning to the intact cell, suggesting that inhibition is not significantly narrowing orientation tuning.

If not lateral inhibition, what makes the width of orientation tuning narrower than that predicted by the map of a simple cell's receptive field? Both Gardner et al. (1999) and Jones and Palmer (1987) hypothesized that orientation tuning could be narrowed by spike threshold. In this scenario, only the largest membrane potential deflections, those evoked by orientations close to the preferred orientation, evoke spikes (Figure 2D), a phenomenon referred to as the "iceberg effect" (Rose and Blakemore, 1974). This hypothesis makes two critical predictions. First, the orientation tuning for spike rate should be significantly narrower than the tuning for membrane potential. This predicted narrowing is shown for a single cell in Figure 2E, and for a population of cells in Figure 2F. The average narrowing (about 3-fold; Figure 2B) is very similar to the average mismatch between tuning width predicted from receptive field maps and tuning width measured from spike rate (Carandini and Ferster, 2000; Volgushev et al., 2000). The second prediction of the iceberg effect is that a simple cell's receptive field map should accurately predict the width of orientation tuning as measured not from spike rate responses (Figure 2B), but from membrane potential responses (Lampl et al., 2001). Receptive field maps for two cells, one with long narrow subfields and one with short, broad subfields are shown in Figure 2G, together with predicted and measured orientation tuning curves of membrane potential responses (Figure 2H). For these cells, and for the population (Figure 2I), measurement and prediction match well. The sharpness of orientation tuning, then, can be accounted for quantitatively by feed-forward geniculo-cortical input to simple cells, as long as the nonlinear effects of threshold are taken into account.

Crossorientation Suppression

The most compelling evidence for lateral inhibition has come from the strong functional interactions between stimuli of different orientation, called crossorientation suppression. In psychophysical experiments, it has been shown that the detectability of one oriented stimulus is lowered by superimposing a second stimulus of the orthogonal orientation (Campbell and Kulikowski, 1966). At the single-cell level, the spike responses of a cortical neuron to a stimulus of the preferred orientation are reduced by superimposing an orthogonal stimulus (Bishop et al., 1973). The responses to high-contrast preferred stimuli can be suppressed by as much as 50%; the responses to low-contrast preferred stimuli can be suppressed almost entirely. It has long been thought that this suppression arises from inhibition between cells with orthogonal preferred orientations. In support of this interpretation, antagonists of $GABA_A$-mediated inhibition reduce crossorientation suppression in visual evoked potentials (Morrone et al., 1987).

Note, however, that more recently bicuculline has been shown to have nonspecific excitatory effects on neurons through its block of Ca^{2+}-activated K^+ (SK) channels (Khawaled et al., 1999). Nor are all the visual response properties of cortical cells consistent with inhibition being the mechanism underlying crossorientation suppression. First, the suppression is largely monocular (Ferster, 1981; Walker et al., 1998); a null-oriented (mask) stimulus presented to one eye has little effect on a preferred (test) stimulus presented to the other eye, whereas the majority of cortical cells, presumably including inhibitory interneurons, are binocular. Second, strong suppression can be evoked by mask stimuli of high temporal frequency, higher than the frequencies to which most cortical cells can respond (Freeman et al., 2002). Third, suppression is insensitive to contrast adaptation, whereas the responses of most cortical cells—presumably including inhibitory interneurons—are strongly suppressed by adaptation (Freeman et al., 2002). Fourth, the onset of suppression is coincident with the onset of neuronal responses, leaving no time for the activation of the inhibitory circuits (Smith et al., 2006). Fifth, as noted above, the evidence from intracellular

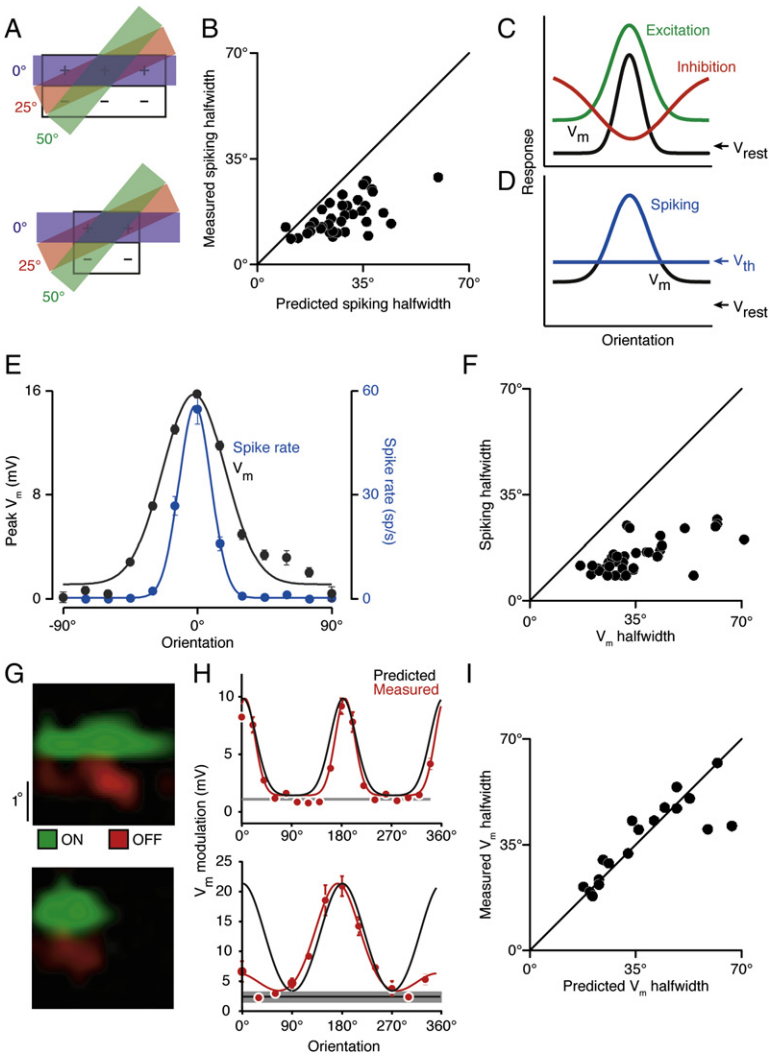

Figure 2. Threshold Narrows Orientation Tuning

(A) Predictions of orientation tuning width from receptive field maps depend on the aspect ratio of the ON and OFF subfields. Long, narrow subfields (top) predict narrower orientation tuning than short subfields (bottom).

(B) A consistent mismatch exists when comparing orientation tuning width predicted from receptive field maps with the measured tuning width to bars or gratings for spiking responses (data replotted from Gardner et al., 1999).

(C and D) Proposed models to account for narrow orientation selectivity. In panel (C), lateral inhibition (red) narrows orientation tuning by suppressing responses to nonoptimal orientations. The resulting Vm tuning curve is narrower than the tuning curve based on excitation alone. In panel (D), the broadly tuned Vm tuning curve is sharpened by spike threshold.

(E and F) Orientation tuning curves for spike rate are consistently narrower than those for membrane potential, as shown for a single cell (E) and across a population of recorded cells (F).

(G and H) Receptive field maps and orientation tuning curves for the membrane potential responses of the two cells. Red, measured from the responses to drifting gratings; black, linear predictions from the receptive field maps in (G). Error bars indicate SEM.

(I) Comparison of the width of predicted and measured orientation tuning for 18 cells. (Compare to [B].)

recording for strong inhibition evoked by stimuli of orthogonal orientation is equivocal. Sixth, an orthogonal stimulus superimposed on a preferred stimulus causes the synaptic inhibition recorded intracellularly in cortical neurons to go down, rather than up. At the same time, synaptic excitation decreases as well (Priebe and Ferster, 2006).

All of these properties of crossorientation suppression are more reminiscent of geniculate relay cells than they are of cortical inhibitory interneurons: relay cells are monocular, respond at high temporal frequency, adapt little to contrast, and by definition respond simultaneously with the excitatory input to the cortex. It has therefore been proposed that crossorientation suppression arises from nonlinear interactions within the relay cell pathway itself (Carandini et al., 2002; Ferster, 1986). One such nonlinearity is synaptic depression: the mask stimulus could increase the level of depression at the synapses between relay cells and cortical cells and thereby reduce the excitatory drive evoked by the test stimulus. Since thalamocortical depression may not be strong enough to account fully for strong crossorientation suppression (Boudreau and Ferster, 2005; Li et al., 2006; Reig et al., 2006), it has also been proposed that crossorientation suppression may arise from two nonlinearities in the responses of relay cells: contrast saturation and firing-rate rectification (Ferster, 1986; Li et al., 2006; Priebe and Ferster, 2006).

To understand how nonlinearities in the feed-forward pathway generate crossorientation suppression, it is useful to consider first how a purely linear model fails to do so (Figure 3). In the linear model, the modulation of a geniculate relay cell's spike rate by a drifting grating is perfectly sinusoidal; a large spontaneous rate prevents the spike rate from ever reaching zero, even during the trough of the response. In addition, the amplitude of the sinusoid is directly proportional to stimulus contrast. For the null-oriented (mask) and preferred (test) grating stimuli, the relay cells respond either out of phase (Figures 3A and 3B; middle column, colored traces) or in phase with one another (Figures 3D and 3E), and the resulting input to the simple cell—which is modeled as the scaled sum of the relay cell responses—is either completely unmodulated or strongly modulated (black traces). Each response, however, has the same mean depolarization.

In response to the superimposed test and mask gratings, the responses of the relay cells differ from one another in both phase and amplitude (Figures 3C and 3F). When the test and mask contrasts are matched (C), the bottom relay cell encounters locations in the plaid stimulus where the dark bars from the two gratings superimpose, alternating with the locations where the bright bars superimpose. The result is a luminance modulation exactly twice as large as that generated by either grating stimulus alone. Since relay cells are assumed here to be linear, the response is therefore twice as large as well. The second relay cell from the top encounters locations in the plaid stimulus where bright bars from one grating superimpose on dark bars from the other. As a result,

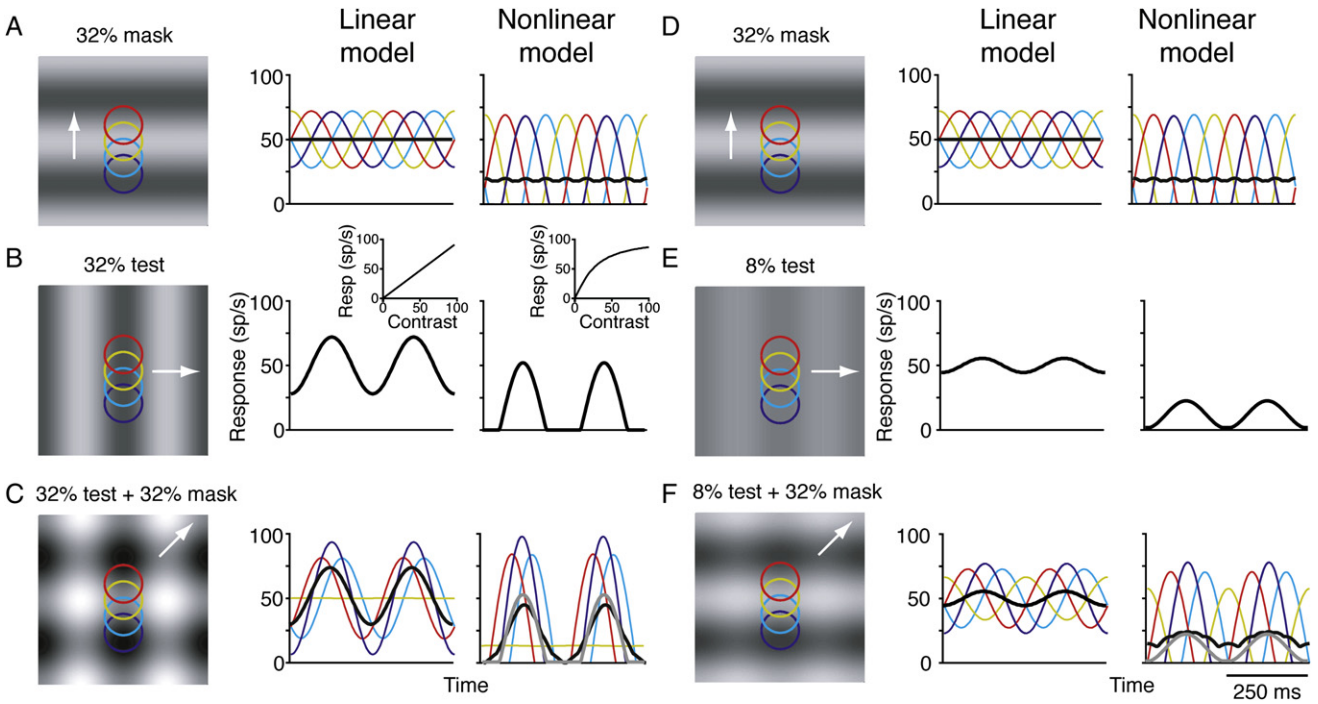

Figure 3. Crossorientation Suppression in Two Feed-Forward Models of a Simple Cell

(A–F) Predicted membrane potential responses are shown for six different grating stimuli. Spiking responses of constituent geniculate relay cells are shown in the colors of their receptive field centers (left). Membrane potential responses of the simple cell are shown in black and are derived from the average of the relay cell responses. In the center in each panel, the responses of the model's constituent geniculate relay cells are assumed to be linear: spontaneous activity is high enough to prevent rectification in the trough of the response, and the amplitude of modulation is proportional to stimulus contrast (inset in [B]). On the right of each panel, spontaneous activity in the relay cells is low, so that the responses rectify, and the amplitude of modulation saturates with increasing contrast (inset in [B]). The linear model predicts that the mask stimulus has no effect on the response to the test stimulus. The nonlinear model predicts that the mask stimulus induces a 15% reduction in the modulation component of the response to the high-contrast test stimulus (compare black traces in [B] and [C]) and 50% reduction in the response to the low-contrast test stimulus (compare [E] and [F]).

there is no modulation of luminance in the relay cell's receptive field, and its response falls to zero. With the response of one relay cell doubling, and the response of another falling to zero, the mask stimulus therefore causes no net change in the feed-forward input evoked by the test stimulus. Some form of inhibition is therefore needed to explain crossorientation suppression.

When contrast saturation and response rectification are introduced into the relay cell responses, the input changes significantly. Now when the plaid is introduced, the response of the third relay cell still falls to zero because its stimulus has zero contrast. The response of the bottom relay cell, however, no longer doubles. Although the mask stimulus doubles the local contrast relative to the test stimulus alone (Figure 3C, left), because the test stimulus was already nearly saturating, the cell's response increases only slightly (right). Altogether then, the mask stimulus causes the total input to the simple cell to fall, in this case by approximately 15%. For low-contrast test gratings (Figure 3F), the mask grating reduces the input to the simple cell (measured here as the amplitude of modulation) by almost 50%. Nearly identical results are obtained when the nonlinear model is based on recorded responses from relay cells instead of rectified sinusoids (Priebe and Ferster, 2006).

This suppression of excitatory relay cell input to simple cells predicted by the nonlinear model (15% for high-contrast test gratings and 50% for low contrast) matches closely what is observed in the membrane potential responses of simple cells: 9% for the high-contrast test grating gratings and 52% for low-contrast (Priebe and Ferster, 2006). To account for the much larger effects observed in cortical spike responses (29% and 89%), only the nonlinearity of spike threshold is needed. Threshold amplifies the effects of the mask gratings in the same way it sharpens orientation tuning. Together with the nonlinearity of relay-cell responses threshold accounts quantitatively for the crossorientation effects in simple cells (Priebe and Ferster, 2006).

Note that while the model accounts for the mask-induced reduction in the modulation component of membrane potential, it also predicts a rise in the mean thalamic input to cortical neurons, and therefore a corresponding rise in mean membrane potential. That a large rise in the mean is not observed experimentally could be explained at least in part by short-term synaptic depression at the thalamocortical synapse (Carandini et al., 2002; Freeman et al., 2002) and because many simple cells receive less than half of their excitatory input from the thalamus (Chung and Ferster, 1998; Ferster et al., 1996).

Contrast-Invariant Orientation Tuning

One remarkable feature of sensory processing is that the perceived qualities of a sensory stimulus are preserved over a wide range of stimulus strength. Visual objects can be recognized over a wide range of illumination and contrast; sounds

can be recognized over a wide range of intensity; odors and tastes can be identified over a wide range of concentration. While changes in stimulus strength generate large changes in the amplitude of neuronal responses, some aspect of the pattern of responses might remain invariant in order for the percept not to change. One simple way to accomplish perceptual invariance, for example, would be to make the ratio of activity in neurons with different preferred stimuli invariant to stimulus strength, which in turn requires that the stimulus tuning of individual neurons be invariant to stimulus strength. Cortical simple cells have exactly this property: the shape and width of their tuning curves for orientation, as well as for other stimulus features, change very little in the face of large changes in stimulus contrast (Alitto and Usrey, 2004; Sclar and Freeman, 1982; Skottun et al., 1987), making these cells a model system for studying the mechanisms of tuning invariance.

Feed-forward models of simple cells have traditionally failed to account for contrast invariance, largely as a consequence of the iceberg effect: increasing the stimulus contrast increases the activity of relay cells at any orientation and thereby increases the synaptic input to the simple cells at every orientation (Figure 4A, left). As the synaptic input scales up, more and more of the tuning curve rises above threshold, and the width of tuning of the spike output should therefore broaden (Figure 4A, right). In addition, in cells with a large proportion of their excitation originating in the lateral geniculate nucleus (LGN), and therefore with a large depolarization at the null orientation, high-contrast stimuli of the nonpreferred orientation will evoke spike responses, whereas low-contrast stimuli at the preferred orientation will evoke none (Figure 4A, red and green points), breaking contrast invariance.

Crossorientation inhibition has long been recognized as a possible solution to this problem. Inhibition tuned to the null orientation would suppress any depolarization and spiking evoked by such stimuli. Threshold can then be lowered so that low-contrast stimuli of the preferred orientation evoke spikes, as is observed in simple cells (Figure 4B). Orientation-independent inhibition (omni-orientation inhibition) from inhibitory cells lacking orientation tuning could also create contrast invariance in spike responses (Martinez et al., 2005; Nowak et al., 2007) (Figure 4C). If the amplitude of inhibition increases with contrast, the orientation tuning curve reaches threshold at the same orientation regardless of stimulus contrast (Troyer et al., 2002).

The feed-forward model and the crossorientation inhibition model make very distinct predictions about the change in membrane potential evoked by null-oriented stimuli. The feed-forward model predicts that because relay cells are not selective for orientation, the mean excitation evoked by null-oriented stimuli should be just as large as that evoked by preferred stimuli (although the peak depolarization at the preferred orientation is much larger). With crossorientation inhibition (either tuned or untuned), the net change in membrane potential evoked by null-oriented stimuli should be 0 or negative. When we tested these predictions in a population of 120 simple cells, the results were not consistent with the presence of strong crossoriented inhibition. That is, null-oriented stimuli were observed to evoke a significant depolarization, on average 43% as large as that evoked at the preferred. For each cell, the amount of null-evoked depolarization was equal to the proportion of excitatory input the cell received from the LGN (Finn et al., 2007). The more excitatory input a cell received from other cortical cells, the less the null-evoked depolarization, presumably because cortical cells are strongly orientation selective and respond little at the null orientation.

How, then, does contrast-invariant orientation tuning emerge, especially in cells like those in Figure 4A (left) that receive most of their excitatory input from relay cells and have a large depolarization at the null orientation? A key component of the answer lies in the trial-to-trial variability of the membrane potential responses and its effect on the relationship between membrane potential and firing rate. Both trial-to-trial variability and moment-to-moment synaptic noise tend to smooth the relationship between average membrane potential and average spike rate so that there is no longer a sharp inflection (see "Spike Threshold and the Power Law" below). Instead, spike rate rises gradually with membrane potential, starting right from the resting membrane potential (Figure 4D). This smoothed V_m-to-spiking transformation narrows orientation tuning curves at all contrasts by approximately the same amount (Anderson et al., 2000b; Hansel and van Vreeswijk, 2002; Miller and Troyer, 2002). One of the surprising consequences of this arrangement is that even at the highest contrast, optimally oriented stimuli barely carry the *trial-averaged* peak membrane potential above threshold. It is the trial-to-trial variability that triggers spikes (Figure 4D; "Spike Threshold and the Power Law").

Even after taking into account the smoothing of the relationship between membrane potential and spike rate, however, contrast invariance will still break down in the feed-forward model at low spike rates (Figure 4D, right); the predicted response to a high-contrast stimulus of the null orientation (green), though small, is still larger than the response to a low-contrast stimulus at the preferred orientation (red). The solution to this problem comes from the observation that trial-to-trial variability of the membrane potential is contrast dependent (Finn et al., 2007). Variability increases with decreasing contrast, and since trial-to-trial variability is partly responsible for carrying the membrane potential above threshold, an increase in variability generates an increase in spikes, even when mean membrane potential is unchanged (see "Spike Threshold and the Power Law" below). As a result, even though a low-contrast stimulus of the preferred orientation evokes a smaller depolarization than a high-contrast stimulus of the null orientation (Figure 4E, left, red and green points), it evokes more spikes (Figure 4E, right). The null stimulus almost never evokes spikes, either because the underlying mean depolarization is too low (low-contrast) or because the trial-to-trial variability is too low (high contrast). Contrast invariance therefore appears in the spike output of simple cells, without lateral inhibition, even when the visually evoked synaptic inputs are themselves not invariant (Finn et al., 2007).

Tuning Dynamics

One prediction of models employing lateral interactions to refine selectivity is that selectivity should evolve over time immediately following the onset of a stimulus. At the beginning of the response, when responses are dominated by feed-forward excitatory inputs, tuning should be broad; later on in the response, as cortical inhibitory circuits become active, tuning should

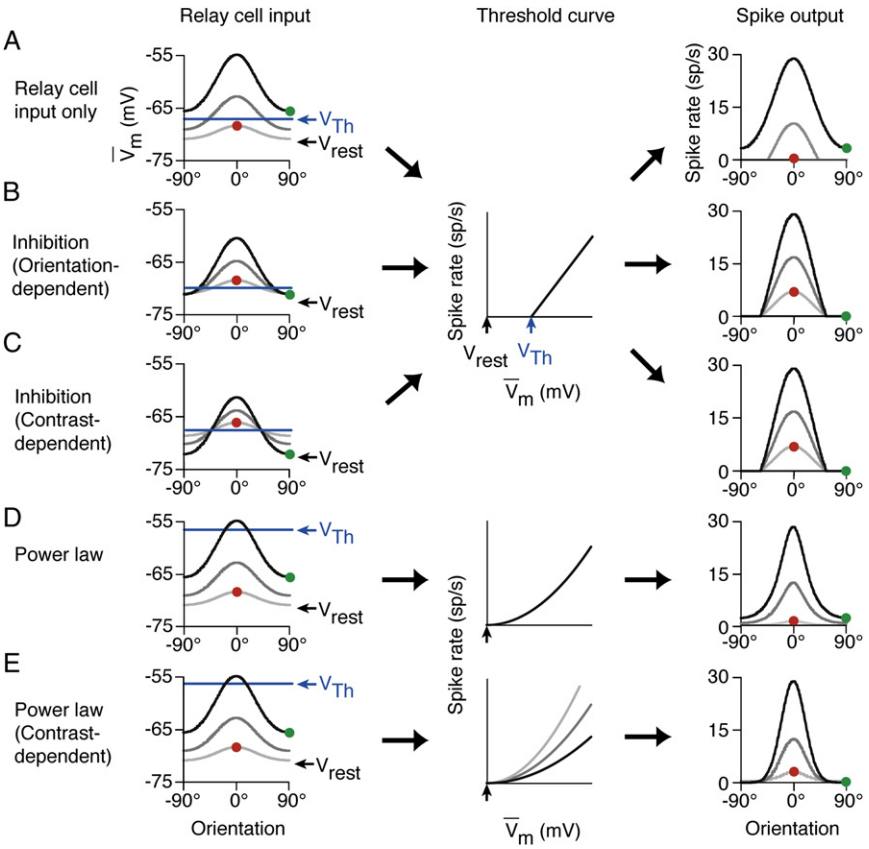

Figure 4. Models of Contrast Invariance of Orientation Tuning

(A) A threshold-linear relationship applied to a feed-forward model. The model assumes input to a simple cell from eight ON-center geniculate relay cells, the behavior of which is based on recordings from the LGN. Orientation tuning curves at three different contrasts are shown. Tuning for spike rate broadens with increasing contrast as more of the tuning curve for membrane potential rises above threshold.

(B) As in (A), but with crossorientation inhibition that cancels geniculate excitation at the null orientation.

(C) As in (A), orientation-untuned inhibition. When the contrast dependence of the inhibition is adjusted properly, the orientation tuning curves for membrane potential all cross threshold at the same point, creating contrast invariance for spike rate.

(D) As in (A), but transformed by a power-law nonlinearity instead of a threshold-linear relationship. Predicted tuning width varies little with contrast in this case, but the amplitude of the response to the orthogonal orientation is larger than the response to the preferred orientation at low contrast.

(E) Contrast invariance of orientation tuning emerges without inhibition when the threshold curve is smoothed by noise and changes gain as a function of contrast (see text).

narrow. Narrowing would also occur if there were a contribution to tuning from the corticothalamic pathway, as suggest by Sillito and Jones (2002).

In extracellular recordings of the responses to rapidly flashed gratings of different orientations, tuning width did narrow over time, but only when the stimuli were several-fold larger than the classical receptive field (Ringach et al., 1997, 2003). Tuning width did not change significantly when the stimuli were limited to the classical receptive field center (Mazer et al., 2002; Xing et al., 2005). In intracellular studies with small stimuli, tuning did not narrow over time, but a decrease in membrane potential appeared at long latencies and all orientations (Gillespie et al., 2001), possibly underlying an observed overall decrease in excitability seen extracellularly (Xing et al., 2005). If any narrowing occurs, then, it is likely to be a consequence of activation of the receptive field surround.

In contrast to orientation selectivity, spatial frequency tuning shows a strong, time-dependent change. While neurons are initially selective for low spatial frequencies, selectivity shifts to high spatial frequencies at longer latencies (Bredfeldt and Ringach, 2002). This "course-to-fine" spatial analysis may originate largely from feed-forward inputs from geniculate relay cells, which show a similar refinement over the course of a response (Allen and Freeman, 2006; Frazor et al., 2004).

Spike Threshold and the Power Law

The solutions to three of the problems we have so far considered—contrast invariance, sharpness of orientation tuning, and crossorientation suppression—are all intimately connected with spike threshold. Threshold explains why receptive field maps do not accurately predict the width of tuning measured from spike rate responses. Threshold significantly amplifies crossorientation suppression for spike rate responses relative to membrane potential responses. Threshold, at least in the form of the iceberg effect, appears to break contrast invariance, but when properly characterized as a contrast-dependent power law, restores invariance. Here, then, we consider the relationship between membrane potential and spike rate in detail and how the power law arises.

The standard threshold-linear curve derives from the instantaneous relationship between membrane potential and spike rate—or as it is usually measured, between injected current and spike rate (Chance et al., 2002; McCormick et al., 1985). In contrast, receptive field properties are almost always measured from the *average* spike rate derived from many stimulus trials, usually in order to increase the signal-to-noise ratio of the measurements. It is in part this averaging that transforms the expected threshold-linear function into a power law (Hansel and van Vreeswijk, 2002; Miller and Troyer, 2002; Priebe et al., 2004); in vivo, the sharp knee of the threshold-linear relationship is smoothed by trial-to-trial variability in neuronal responses (Anderson et al., 2000b).

This smoothing is shown for a simple cell in Figure 5. Cycle-averaged spike-rate responses to three different stimuli are shown in Figures 5A–5C, averaged membrane potential superimposed on single-trial responses in D–F, and average membrane

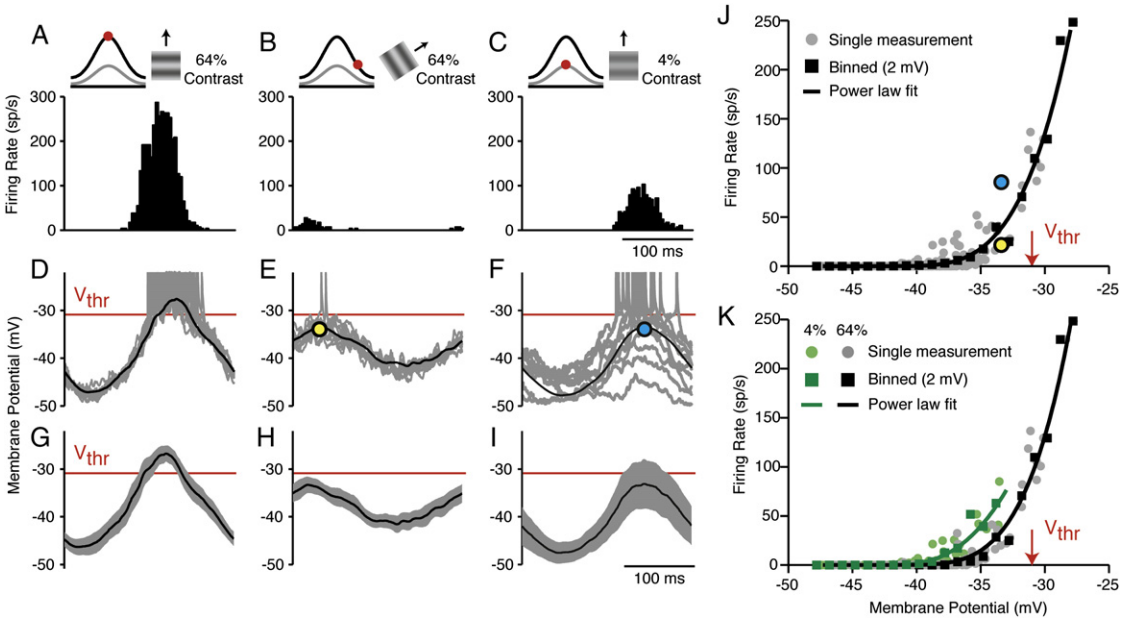

Figure 5. Contrast Dependence of Trial-to-Trial Variability and Its Effect on the Relationship between Membrane Potential and Spike Rate
(A–C) Spike-rate responses of a simple cell to three different grating stimuli.
(D–F) Corresponding membrane potential responses. Several superimposed trials are shown (gray) along with the average response (black). At high contrast (D and E), the trial-to-trial variability is low compared to low contrast (F).
(G–I) Average membrane potential responses (black), with trial-to-trial standard deviation at each point in tine shown as gray shading.
(J) Relationship between membrane potential and spike rate for average membrane potential and spike rate. Gray points are taken from 30 ms epochs of the averaged responses. Yellow and blue points correspond to those in (E) and (F), showing that higher trial-to-trial variability leads to higher spike rate, even when the mean potential is the same. Black points are averages of the gray points in 2 mV intervals. Curve is a fit of the gray points to a power law (Equation 1).
(K) Same data as in (J), but sorted by stimulus contrast.

potential with superimposed trial-to-trial standard deviation in G and H. The membrane potential and spike rate are then measured at 30 ms intervals from the cycle-averaged responses and plotted against one another in Figure 5J (gray points). There are two striking features in this graph. The first is the large scatter. Points with identical mean potential can have very different mean spike rates. Second, the mean spike rate can be non-zero for mean potentials that lie far below the biophysical spike threshold. Both features are the result of trial-to-trial variability. In Figure 5F, for example, the mean potential (black) never rises above threshold, and yet many individual traces do, giving rise to a non-zero spike rate during part of the response (Figure 5C). In other words, the trial-to-trial variability, as well as the mean potential, is critical in determining the average firing rate (Azouz and Gray, 2003). As a consequence, portions of the responses that have identical means but very different variability have very different firing rates. Compare, for example, the peaks of the traces in Figures 5E and 5F (blue and yellow symbols), and the corresponding points in F.

As shown by the solid curve in Figure 5J, the relationship between average membrane potential and average spike rate can be well approximated by a power law (Hansel and van Vreeswijk, 2002; Miller and Troyer, 2002; Priebe et al., 2004):

$$R(V_m) = k[\bar{V}_m - V_{rest}]_+^p \quad (1)$$

where R is the spike rate, V_m is the membrane potential, k is a gain factor, V_{rest} is the resting membrane potential, and p is the exponent of the power law, which usually lies between 2.5 and 5. The solid curve in Figure 5 falls closely along the black points in the figure, which represent the average of individual (gray) points in 2 mV intervals (Finn et al., 2007; Priebe and Ferster, 2005, 2006; Priebe et al., 2004).

Note that the variables in Equation 1, k and p, depend on the distance between V_{rest} and the biophysical threshold and on the amplitude of the trial-to-trial variability (Hansel and van Vreeswijk, 2002; Miller and Troyer, 2002). While the power law is mathematically convenient, however, it holds no theoretical significance and is not the only function that will fit the data reasonably well. Equation 1 is a specific form of a more general equation (Carandini and Ferster, 2000; Movshon et al., 1978) relating average membrane potential to average spike rate in the form:

$$R(V_m) = k[\bar{V}_m - V_{th}]_+^p. \quad (2)$$

V_{th} can be chosen to be anywhere in the range between resting membrane potential and biophysical spike threshold. For example, with p set to 1 and V_{th} to biophysical threshold, the equation describes the standard threshold-linear relationship. Neither the resulting sharp inflection at V_{th} nor the region between V_{rest} and V_{th} with 0 spike rate, however, is observed in intracellular data (Figure 5). Setting V_{th} to V_{rest} and p greater than 1 (Equation 1) gives a better match to the average data.

By fitting Equation 1 to all responses with a single pair of values for p and k, we implicitly make the assumption that

trial-to-trial variability and biophysical threshold are invariant across stimuli. One stimulus attribute that leads to consistent changes in trial-to-trial variability, however, is stimulus contrast, or strength: as contrast increases—independent of orientation—variability decreases. This trend can be seen for two stimuli by comparing Figures 5E and 5F. In a population of 52 simple cells, measuring across all stimulus orientations, the standard deviation of the membrane potential at the peak response was on average 38% higher at low contrast than at high contrast (Finn et al., 2007). As a result, the number of spikes associated with a given mean membrane potential was on average greater at low contrast than at high contrast (Figure 5K). In other words, p and k in Equation 1 vary systematically with contrast. As discussed above, this contrast dependence is critical in preserving contrast invariance of orientation tuning, and perhaps of other parameters.

Direction Selectivity

In addition to orientation selectivity, visual cortical neurons express a number of other receptive field properties, many of which have been attributed to lateral inhibition. We will consider the contribution of lateral inhibition and spike threshold to direction selectivity, surround suppression (size tuning), and the distinction between simple and complex cells.

The bias for direction selectivity in the excitatory input to simple cells is thought to arise from the properties of the LGN afferents (Saul and Humphrey, 1992). Relay cell inputs to different locations within the subfields of simple cells respond with different latencies, creating a spatial gradient of latency across the receptive field in the direction perpendicular to the preferred orientation (Figure 6A) (Adelson and Bergen, 1985; Watson and Ahumada, 1983). This latency gradient causes the cortical cell to prefer motion in the direction of decreasing latency. That is, a direction-selective cortical neuron will receive synchronous, and therefore maximal, excitation from all regions of its receptive field only when the different regions are activated in the proper order by a moving stimulus, starting from the longest latency region and proceeding toward the shortest (Figure 6A, leftward bar). When the stimulus moves in the opposite direction, the excitation will be asynchronous, reducing the response of a cell (Figure 6A, rightward bar). The bias created by this mechanism, when amplified by threshold, can give rise to the complete direction selectivity observed in many cortical cells.

In parallel with orientation selectivity, linear models underestimate the degree of direction selectivity that is measured from spike rate responses to moving stimuli. That is, the direction selectivity of most cells is far higher than linear predictions based on measured latency gradient (Albrecht and Geisler, 1991; DeAngelis et al., 1993a, 1993b; Mclean and Palmer, 1988; Reid et al., 1987, 1991; Tolhurst and Dean, 1991). The direction selectivity indices for many simple cells' spike responses

$$\left(DI = \frac{R_{pref} - R_{null}}{R_{pref} + R_{null}}\right)$$

are at or near 1 (complete selectivity), whereas the selectivity predicted from the latency gradients is rarely above 0.5. Here, inhibition evoked by the nonpreferred stimuli could again explain the nonlinear behavior of the cells (Torre and Poggio, 1978), a proposal that was supported by the discovery of strong, visually evoked shunting inhibition in direction-selective retinal ganglion cells and in cortical cells (Borg-Graham et al., 1998). Recent experiments, however, have shown that visually evoked inhibition in cortical cells does not have the correct stimulus selectivity to enhance direction selectivity. Instead, inhibition, like excitation, is larger in response to motion in the preferred direction than in response to motion in the opposite direction (Priebe and Ferster, 2005).

That spike threshold can explain the mismatch between linear predictions and measured direction selectivity is shown in Figures 6B–6E. The spatiotemporal maps of the receptive field, which show the gradient in latency, accurately predict the direction selectivity of the synaptic input to the cell as reflected in membrane potential (Figures 6C–6E). Threshold then amplifies the selectivity of the input to generate the dramatically increased selectivity of the spike output (Figure 6E) (Jagadeesh et al., 1993; Priebe and Ferster, 2005).

These experiments do not rule out the possibility that null-directed inhibition operates at later stages of the cortical circuit. Suppressive filters tuned to the null direction have been identified in extracellular records from complex cells of the primate visual cortex, for example (Rust et al., 2005), although it is not yet clear how these suppressive filters are related to synaptic inhibition.

Size Tuning (Lateral Inhibition in the Spatial Domain)

A receptive field is defined as those locations in visual space where a stimulus elicits a change in activity (Kuffler, 1953). Historically, receptive fields have almost invariably been measured from spike rate. But here, the iceberg effect operates as well: the receptive field measured from membrane potential responses is larger than that measured from spikes, so there are regions outside the spike-defined receptive field in which stimuli evoke subthreshold responses (Bringuier et al., 1999). In addition, many cells exhibit a receptive field surround in which stimuli suppress the response to a preferred stimulus within the receptive field (Anderson et al., 2001; Angelucci et al., 2002; Blakemore and Tobin, 1972; Cavanaugh et al., 2002a, 2002b; DeAngelis et al., 1994; Levitt and Lund, 1997; Li and Li, 1994; Ozeki et al., 2004). Although relay cells are themselves surround suppressed (Sillito et al., 1993), a significant component of the cortical suppression is likely cortical in origin. First, a component of cortical suppression is orientation selective; maximal suppression is evoked by surround stimuli that match the cell's preferred orientation. Second, there is a delay between the center response and the appearance of suppression (Bair et al., 2003).

Surround suppression, then, is an example of intracortical lateral inhibition in the spatial domain, and except for its orientation selectivity, is much like the retinal lateral inhibition first described by Hartline (1949). A number of experiments, however, lead us to suggest that the mechanism underlying surround suppression differs fundamentally from retinal lateral inhibition. In classical lateral inhibition, suppression of the recorded cell is mediated by synaptic inhibition. In cortical surround suppression, the surround stimulus instead decreases synaptic excitation and

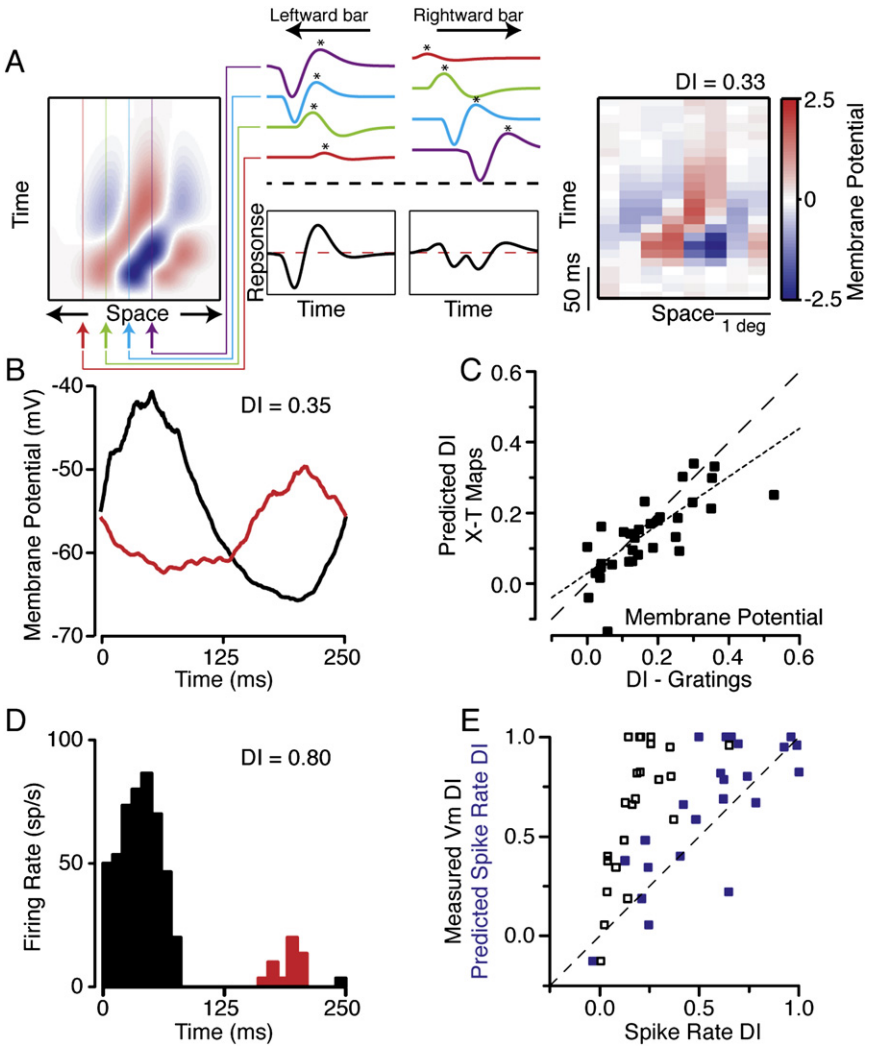

Figure 6. Linear Predictions of Direction Selectivity

(A) Mapping receptive fields in space and time. An idealized X-T map of a simple cell receptive field is shown in the left panel. Colored traces correspond the response to a stimulus flashed at the locations indicated by the arrows in left panel. The responses are shifted in time to simulate the temporal relationship that would result from a stimulus moving through the receptive field leftward or rightward. The sum of the responses (black) indicates what the membrane potential response in the simple cell will be. An X-T map recorded from a simple cell in response to flashing bar stimuli is shown in the right panel.

(B) Membrane potential and (D) spike rate responses of the same simple cell to drifting gratings of the preferred (black) and null (red) direction.

(C) Direction index for membrane potential responses to gratings plotted against direction index predicted from X-T maps.

(E) Direction index for spike rate plotted against the index for membrane potential (black, open symbols) and against a prediction of spike rate made by passing the recorded membrane potential through the measured relationship between membrane potential and spike rate for each cell (blue, closed symbols) (Equation 1).

inhibition (H. Ozeki and D.F, 2005, Soc. Neurosci., abstract, 389.20). In addition, applying $GABA_A$ antagonists to a cell has minimal effect on cortical surround suppression (Ozeki et al., 2004). These and other observed properties of surround suppression have led us to suggest that it depends on the cortex operating as an inhibition-stabilized network (Tsodyks and Markram, 1997). This mechanism still requires an inhibitory connection in which laterally projecting excitatory neurons synapse onto local inhibitory interneurons. But in an inhibition-stabilized network, activating the surround pathway will paradoxically lead to the observed decrease in activity in both the excitatory and inhibitory neurons within the network (H. Ozeki, E. Shafer, K.D. Miller, and D.F., unpublished data), giving rise to the same suppressive effects that classical lateral inhibitory circuits would.

The Classification of Simple and Complex Cells

Not only does spike threshold sharpen feature selectivity in cortical neurons, it also sharpens the distinction between cells of different classes. Simple cells, by definition, have segregated ON and OFF subregions in their receptive fields (Hubel and Wiesel, 1962), generated by segregated input from ON and OFF relay cell input (Alonso et al., 2001). As a result, when a grating drifts across the receptive field, the response is strongly modulated at the grating temporal frequency. That is, the modulation component of the response (R_1) is large relative to the mean elevation in firing (R_0). Complex cell receptive fields, by definition, have no subregions (Hubel and Wiesel, 1962) and are constructed at least in some cases from the input of multiple simple cells (Alonso and Martinez, 1998). Complex cell responses are therefore only weakly modulated and have a small R_1 relative to R_0. The modulation ratio, R_1/R_0, in a large population of cortical cells forms a clearly bimodal distribution, with simple cells having ratios greater than one and complex cells less than one (Skottun et al., 1991). This bimodal distribution has been taken as evidence that the two groups form fundamentally distinct populations and that their underlying synaptic connectivity—originating predominantly either from relay cells or from simple cells—is equally distinct. Support for this view comes from the reported laminar segregation of the two cell types, with simple cells lying only in the thalamic input layers, IV and VI (Martinez et al., 2005); but see Ringach et al. (2002) and Jacob et al., 2003, Soc. Neurosci., abstract, 910.13.

If the synaptic connectivity underlying simple and complex cells were distinct, then this distinction should be evident in the cells' membrane potential responses. In one series of experiments, cortical cells did divide into two distinct populations on the basis of the degree of overlap between ON and OFF membrane potential responses (Martinez et al., 2005). We have found, however, that the sharp division of simple and complex cells

measured both from an overlap index and from the modulation ratio is not evident in membrane potential responses (Priebe et al., 2004). For membrane potential, the modulation ratio (V_1/V_0) forms a unimodal distribution instead of a bimodal distribution (Figure 7B, bottom). The majority of complex cells have lower modulation ratios than simple cells, but there is overlap between the two populations. As predicted by Mechler and Ringach (2002), spike threshold acts to sharpen the distinction between simple and complex cells.

As shown in Figure 7, the complex relationship between V_1/V_0 and R_1/R_0 depends on the nonlinear interactions between three factors: the exponent, p, of the power law in Equation 1, the size of the membrane potential modulation (V_1), and the size of the mean depolarization (V_0). For small values of V_1/V_0 (0–0.8), spike threshold amplifies the modulation ratio significantly because the peak of the membrane potential modulation is amplified more than the mean or trough. For large values of V_1/V_0 (0.8–2.0), R_1/R_0 saturates, and so threshold has little effect (Figure 7A). This saturation compresses the long tail of V_1/V_0 distribution into a peak in the R_1/R_0 distribution in the range of 1–2 (Figure 7B). Thus, the exact shape of the distribution of V_1/V_0 (the peak and long tail) interacts in a very specific way with the shape of the transformation between V_1/V_0 and R_1/R_0 (initial amplification and later saturation). Both properties—one of which depends on the intrinsic properties of the neurons and one of which depends on the underlying synaptic connectivity of the neurons—are necessary to make the final, bimodal shape of the R_1/R_0 distribution and create the clear-cut distinction between simple and complex cells evident in spike-rate measurements (Priebe et al., 2004).

Inhibition and Threshold in Auditory and Somatosensory Cortex

In sensory modalities other than vision, the best evidence for lateral inhibition comes from the sensory periphery or from subcortical structures. In the auditory brainstem, the fine selectivity for interaural time differences that underlie sound localization depends on inhibition (D'Angelo et al., 2005; Fujita and Konishi, 1991; Park et al., 1997). Bat-call selectivity and frequency tuning in the inferior colliculus (Xie et al., 2005; Yang et al., 1992) and the auditory thalamus (Olsen and Suga, 1991; Suga et al., 1997) are diminished by blocking inhibition. Whether inhibition shapes selectivity in the auditory cortex is less clear. Blocking inhibition with bicuculline application does cause frequency tuning curves to broaden (Wang et al., 2000, 2002), which may also be a result of the network becoming unstable, rather than because inhibition is tightening tuning. From intracellular recordings, it appears that excitation and inhibition match in tuning for tone intensity and frequency (Zhang et al., 2003), similar to what we have found in visual cortex for contrast and orientation. Also, in parallel with the orientation selectivity in visual cortex, the tuning width for tone frequency is broader for membrane potential than for spike rate (Tan et al., 2004). While feature selectivity is matched for excitation and inhibition, the relative timing is not: inhibition usually follows excitation by 1–4 ms, shortening the response relative to the duration of the excitatory input (Wehr and Zador, 2003). Similar, though slower, sequences of excitation and inhibition are seen in visual cortical responses to flashed stimuli.

Analogous results have been reported for the somatosensory cortex, particularly in the whisker-barrel cortex of rodents. These cortical neurons are tuned to respond almost exclusively to the principal whisker and are tuned for the direction of deflection of the principle whisker. Both types of tuning are weaker in membrane potential responses than in spike-rate responses (Brecht et al., 2003; Moore and Nelson, 1998). Tuning of the excitatory input is thought to originate in the tuning of thalamic afferents. Inhibition has similar, though somewhat broader tuning for adjacent whiskers. This broadly tuned inhibition could arise from convergence of inputs from multiple barrels or from inhibitory neurons within a barrel that are more broadly tuned than excitatory neurons (Kelly et al., 1999; Swadlow, 2002, 2003; Swadlow et al., 1998). For brief, impulse-like stimuli, excitation and inhibition follow a similar time course to that observed in auditory cortex: excitation precedes inhibition, allowing a brief window in time in which spikes may be evoked (Cruikshank et al., 2007; Higley and Contreras, 2006).

Discussion

The pioneering work of physiologists beginning in the 1940s leaves little doubt that, in the periphery, inhibition refines the selectivity of sensory neurons. It has seemed a natural extension to assume that inhibition does the same in sensory cortex. The many nonlinear stimulus interactions in cortical responses, such as crossorientation suppression, seem to have all the hallmarks of lateral inhibition. And numerous experiments, such as the inactivation of $GABA_A$-mediated inhibition, seem to confirm the existence of cortical lateral inhibition. In this review, however, we demonstrate that, in generating the exquisite selectivity of cortical cells, the function of lateral inhibition is taken over by a number of simple, well-defined nonlinearities of visual neurons. Spike threshold sharpens selectivity for orientation (Azouz and Gray, 2003; Carandini and Ferster, 2000; Volgushev et al., 2000) and direction (Jagadeesh et al., 1993; Priebe and Ferster, 2005) in visual cortex, for frequency in auditory cortex (Tan et al., 2004), and for whiskers in somatosensory cortex (Brecht et al., 2003; Moore and Nelson, 1998). In addition, in visual cortex, threshold amplifies the effects of masking (Priebe and Ferster, 2006), amplifies surround suppression (Anderson et al., 2001), enhances the distinction between simple and complex cells (Priebe et al., 2004), increases ocular dominance, and sharpens both spatial and temporal frequency tuning (N.J.P. and D.F., unpublished data).

These findings have important implications for cortical circuitry and its development. Because of the nonlinearity of the V_m-to-spike-rate transformation, narrow tuning or complete selectivity for any stimulus feature such as orientation or direction can emerge from excitatory inputs that are only broadly tuned or weakly biased. Similarly, complete crossorientation suppression or surround suppression requires only a 50% reduction in feed-forward excitatory inputs. In other words, the functional specificity of thalamic and cortical synaptic inputs to a cell can be much less precise than one might first expect from the cell's selectivity; threshold and the other nonlinear properties of the visual pathways that we have considered will effectively filter out many of the functional consequences of imprecise connections. Thus, the constraints that apply during development of the

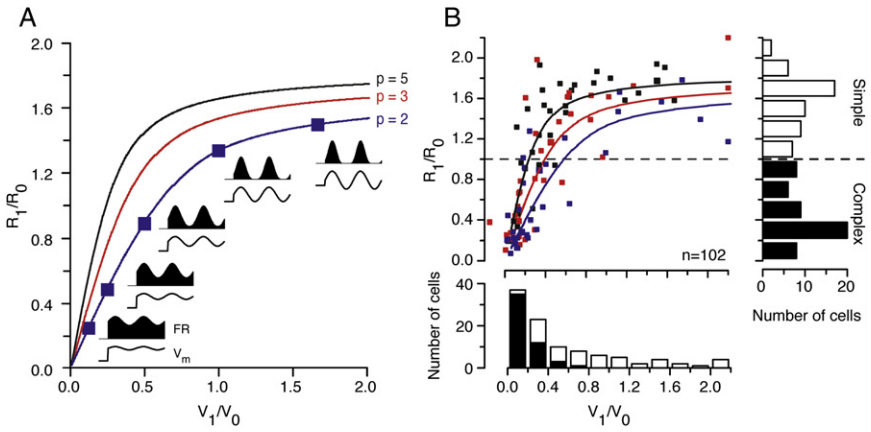

Figure 7. Threshold and the Segregation of Simple and Complex Cells

(A) The predicted relationship between R_1/R_0, the ratio of the modulation and mean components of spike rate, and V_1/V_0, the ratio for membrane potential. Curves are shown for three different values of *p*, the exponent in the power-law relationships between membrane potential and spike rate (Equation 1). Membrane potential traces and spike rate histograms with different ratios are shown at various points in the graph.

(B) R_1/R_0 plotted against V_1/V_0 for a population of recorded simple cells. Points are color coded for different ranges of the exponent, *p*. Solid curves taken from (A). Histograms for the two ratios are shown below and to the right.

cortical circuit may not be as strict as they might first seem from descriptions of neuronal selectivity.

That spike threshold refines selectivity is not a novel concept. Numerous computational models have proposed that some output nonlinearity like an iceberg effect or power law is necessary to account for the responses of cortical neurons (Gardner et al., 1999; Heeger, 1993; Jones and Palmer, 1987; Rose and Blakemore, 1974; Tolhurst and Heeger, 1997). What is surprising is how pervasive the effects of threshold are, that stimulus-specific features such as crossorientation suppression can arise from basic stimulus-blind nonlinearities such as threshold and response rectification.

In addition to the refinement of selectivity, a critical function that has often been assigned to inhibition is gain control or normalization. Normalization by contrast-dependent, shunting inhibition from recurrent intracortical connections has been proposed to account for many nonlinear features of cortical responses (Carandini et al., 1997; Heeger, 1992). Even for gain control, however, threshold—in combination with contrast-dependent changes in trial-to-trial variability—can fulfill some of the function normally assigned to inhibition (Azouz and Gray, 2003; Carandini, 2007).

Spike threshold strongly affects the transmission of information through sensory cortex. Because the majority of cortical neurons are generally silent in the absence of a stimulus, and the resting membrane potential lies far below threshold, relatively large deviations in the membrane potential are required to generate spikes, and information encoded in small deviations can be lost (Ringach and Malone, 2007). In the periphery, where neurons have large background firing rates, small increases and decreases in membrane potential are transduced into detectable changes in firing rate. While it may be important in the periphery to transmit as much information as possible to cortex with high fidelity, the central goal for cortical neurons is likely not limited to information transmission, but extends to the transformation of information into the increasingly specific representations that facilitate perception and cognition. Retinal and LGN neurons, then, respond to stimuli of almost any shape, and their responses are smoothly modulated by stimulus contrast or strength; neurons in V1 are narrowly tuned for stimulus orientation, size, and direction, but their contrast-response functions saturate at fairly low contrasts. Clearly, spike threshold is fundamental for these refinements in selectivity and for generating the sparse cortical representation.

The Function of Cortical Inhibition

If spike threshold performs so many functions related to the refinement of receptive field properties, what then does inhibition contribute to cortical computation? In V1, maximal inhibition is most often evoked by stimuli of the preferred orientation (Ferster, 1986; Douglas et al., 1991; Hirsch et al., 1998). In simple cells, a large fraction of this inhibition is arranged in a so-called push-pull organization. In each subfield, a stimulus of the optimal polarity (a bright bar in an ON region or a dark bar in an OFF region) evokes strong excitation from geniculate relay cells ("push"); a stimulus of the opposite polarity causes a withdrawal of excitation by suppressing the spontaneous activity of the relay cells. This withdrawal, however, is limited in size given that the firing rates of geniculate neurons can never go below zero. Since LGN firing rates can rise much farther than they can fall, the result is an asymmetry between the excitatory responses to oppositely directed stimuli. It may be for this reason that the withdrawal of relay cell input evoked by suppressive stimuli is accompanied by strong synaptic inhibition ("pull") (Ferster, 1988; Heggelund, 1986; Hirsch et al., 1998; Hubel and Wiesel, 1962; Palmer and Davis, 1981). This push-pull inhibition effectively linearizes the cell's responses by creating a more precise opposition between the effects of facilitatory and suppressive stimuli. It is rare, in fact, for the depolarizing and hyperpolarizing phases of the responses to be perfectly balanced: the latter are invariably larger, most likely because of the asymmetry in the driving forces on excitatory and inhibitory currents. But the large amplitude of the inhibitory conductance ensures that the excitability of simple cells is strongly suppressed by stimuli of the wrong polarity. Complex cells, like simple cells, are maximally inhibited by stimuli of the preferred orientation. There is no analog of push-pull inhibition for complex cells, however, and so the function of this inhibition is not clear.

Inhibition may also be acting to control the timing of responses in cortical networks. While excitation and inhibition are generally tuned for the same stimulus parameters, their latencies differ, in part because excitation arises directly from the thalamus, whereas inhibition is mediated by intracortical inhibitory interneurons. The delayed, long-lasting inhibition, a common feature

of many areas of the brain, can thereby shorten what would otherwise be a long excitatory potential, and increase the temporal precision of cortical responses. This feature points out a significant difference between sensory modalities: the excitation-inhibition sequence evoked by brief stimuli is several fold faster in auditory cortex (Wehr and Zador, 2003) and somatosensory cortex (Cruikshank et al., 2007; Higley and Contreras, 2006) than it is in visual cortex (Boudreau and Ferster, 2005; Hirsch et al., 1998). This difference seems more likely to be a function of the timing of the afferent activity that drives the cortex, rather than an intrinsic difference in circuitry, since electrical stimulation of the LGN evokes a rapid excitation-inhibition sequence similar to the ones evoked by natural stimulation in auditory and somatosensory cortex (Douglas and Martin, 1991; Ferster and Lindström, 1983).

In addition, inhibition is likely required to maintain the cortical circuit in a stable state. The more inhibition present in the circuit, the stronger the excitatory recurrent connections can be and still prevent runaway feedback excitation in the excitatory network (Douglas and Martin, 1991). Strong excitatory recurrence in turn increases the dynamic range of cortical neurons, increases their information-carrying capacity, and increases the ability of the cortex to perform complex computations (Hansel and Sompolinsky, 1996; Latham and Nirenberg, 2004; Tsodyks et al., 1997; van Vreeswijk and Sompolinsky, 1998). Finally, balanced excitation and inhibition could help generate the irregular temporal patterns of firing observed in cortical neurons (Shadlen and Newsome, 1998).

Conclusion

Since Hubel and Wiesel first described orientation selectivity, two strikingly different theories on cortical computation have emerged. In one, cortex is envisioned as a passive filter, simply summing the feed-forward afferent excitation to create transformations in the representation of the world. This perspective is one in which an orientation column forms the basic computational unit of the cortex, with each unit operating more or less independently from its neighbors. The alternative theory proposes that intracolumnar interactions, in the form of lateral inhibition, are essential to cortical computation. Using layer 4 of V1 as a model system for the study of cortical computation, we have provided strong evidence that a columnar, feed-forward perspective, with the known nonlinearities of individual neurons, can account for the essentials of cortical response selectivity.

ACKNOWLEDGMENTS

The authors wish to thank Kenneth D. Miller, Wilson S. Geisler, Jessica L. Hanover, and Judith A. Hirsch for helpful comments on the manuscript.

REFERENCES

Adelson, E.H., and Bergen, J.R. (1985). Spatiotemporal energy models for the perception of motion. J. Opt. Soc. Am. *2*, 284–299.

Albrecht, D.G., and Geisler, W.S. (1991). Motion selectivity and the contrast-response function of simple cells in the visual cortex. Vis. Neurosci. *7*, 531–546.

Alitto, H.J., and Usrey, W.M. (2004). Influence of contrast on orientation and temporal frequency tuning in ferret primary visual cortex. J. Neurophysiol. *91*, 2797–2808.

Allen, E.A., and Freeman, R.D. (2006). Dynamic spatial processing originates in early visual pathways. J. Neurosci. *26*, 11763–11774.

Alonso, J.M., and Martinez, L.M. (1998). Functional connectivity between simple cells and complex cells in cat striate cortex. Nat. Neurosci. *1*, 395–403.

Alonso, J.M., Usrey, W.M., and Reid, R.C. (2001). Rules of connectivity between geniculate cells and simple cells in cat primary visual cortex. J. Neurosci. *21*, 4002–4015.

Anderson, J.S., Carandini, M., and Ferster, D. (2000a). Orientation tuning of input conductance, excitation, and inhibition in cat primary visual cortex. J. Neurophysiol. *84*, 909–926.

Anderson, J.S., Lampl, L., Gillespie, D., and Ferster, D. (2000b). The contribution of noise to contrast invariance of orientation tuning in cat visual cortex. Science *290*, 1968–1971.

Anderson, J.S., Lampl, I., Gillespie, D.C., and Ferster, D. (2001). Membrane potential and conductance changes underlying length tuning of cells in cat primary visual cortex. J. Neurosci. *21*, 2104–2112.

Angelucci, A., Levitt, J.B., Walton, E.J., Hupe, J.M., Bullier, J., and Lund, J.S. (2002). Circuits for local and global signal integration in primary visual cortex. J. Neurosci. *22*, 8633–8646.

Azouz, R., and Gray, C.M. (2003). Adaptive coincidence detection and dynamic gain control in visual cortical neurons in vivo. Neuron *37*, 513–523.

Bair, W., Cavanaugh, J.R., and Movshon, J.A. (2003). Time course and time-distance relationships for surround suppression in macaque V1 neurons. J. Neurosci. *23*, 7690–7701.

Ben-Yishai, R., Bar-Or, R.L., and Sompolinsky, H. (1995). Theory of orientation tuning in visual cortex. Proc. Natl. Acad. Sci. USA *92*, 3844–3848.

Bishop, P.O., Coombs, J.S., and Henry, G.H. (1973). Receptive fields of simple cells in the cat striate cortex. J. Physiol. *231*, 31–60.

Blakemore, C., and Tobin, E.A. (1972). Lateral inhibition between orientation detectors in the cat's visual cortex. Exp. Brain Res. *15*, 439–440.

Borg-Graham, L.J., Monier, C., and Fregnac, Y. (1998). Visual input evokes transient and strong shunting inhibition in visual cortical neurons. Nature *393*, 369–373.

Boudreau, C.E., and Ferster, D. (2005). Short-term depression in thalamocortical synapses of cat primary visual cortex. J. Neurosci. *25*, 7179–7190.

Brecht, M., Roth, A., and Sakmann, B. (2003). Dynamic receptive fields of reconstructed pyramidal cells in layers 3 and 2 of rat somatosensory barrel cortex. J. Physiol. *553*, 243–265.

Bredfeldt, C.E., and Ringach, D.L. (2002). Dynamics of spatial frequency tuning in macaque V1. J. Neurosci. *22*, 1976–1984.

Bringuier, V., Chavane, F., Glaeser, L., and Fregnac, Y. (1999). Horizontal propagation of visual activity in the synaptic integration field of area 17 neurons. Science *283*, 695–699.

Brosch, M., and Schreiner, C.E. (1997). Time course of forward masking tuning curves in cat primary auditory cortex. J. Neurophysiol. *77*, 923–943.

Calford, M.B., and Semple, M.N. (1995). Monaural inhibition in cat auditory cortex. J. Neurophysiol. *73*, 1876–1891.

Campbell, F.W., and Kulikowski, J.J. (1966). Orientational selectivity of the human visual system. J. Physiol. *187*, 437–445.

Carandini, M. (2007). Melting the iceberg: contrast invariance in visual cortex. Neuron *54*, 11–13.

Carandini, M., and Ferster, D. (2000). Membrane potential and firing rate in cat primary visual cortex. J. Neurosci. *20*, 470–484.

Carandini, M., Heeger, D.J., and Movshon, J.A. (1997). Linearity and normalization in simple cells of the macaque primary visual cortex. J. Neurosci. *17*, 8621–8644.

Carandini, M., Heeger, D.J., and Senn, W. (2002). A synaptic explanation of suppression in visual cortex. J. Neurosci. *22*, 10053–10065.

Cavanaugh, J.R., Bair, W., and Movshon, J.A. (2002a). Nature and interaction of signals from the receptive field center and surround in macaque V1 neurons. J. Neurophysiol. *88*, 2530–2546.

Cavanaugh, J.R., Bair, W., and Movshon, J.A. (2002b). Selectivity and spatial distribution of signals from the receptive field surround in macaque V1 neurons. J. Neurophysiol. *88*, 2547–2556.

Chance, F.S., Abbott, L.F., and Reyes, A.D. (2002). Gain modulation from background synaptic input. Neuron *35*, 773–782.

Chapman, B., Zahs, K.R., and Stryker, M.P. (1991). Relation of cortical cell orientation selectivity to alignment of receptive fields of the geniculocortical afferents that arborize within a single orientation column in ferret visual cortex. J. Neurosci. *11*, 1347–1358.

Chung, S., and Ferster, D. (1998). Strength and orientation tuning of the thalamic input to simple cells revealed by electrically evoked cortical suppression. Neuron *20*, 1177–1189.

Creutzfeldt, O.D. (1977). Generality of the functional structure of the neocortex. Naturwissenschaften *64*, 507–517.

Crook, J.M., Kisvarday, Z.F., and Eysel, U.T. (1998). Evidence for a contribution of lateral inhibition to orientation tuning and direction selectivity in cat visual cortex: reversible inactivation of functionally characterized sites combined with neuroanatomical tracing techniques. Eur. J. Neurosci. *10*, 2056–2075.

Cruikshank, S.J., Lewis, T.J., and Connors, B.W. (2007). Synaptic basis for intense thalamocortical activation of feedforward inhibitory cells in neocortex. Nat. Neurosci. *10*, 462–468.

Crutch, S.J., and Warrington, E.K. (2001). Refractory dyslexia: evidence of multiple task-specific phonological output stores. Brain *124*, 1533–1543.

D'Angelo, W.R., Sterbing, S.J., Ostapoff, E.M., and Kuwada, S. (2005). Role of GABAergic inhibition in the coding of interaural time differences of low-frequency sounds in the inferior colliculus. J. Neurophysiol. *93*, 3390–3400.

DeAngelis, G.C., Ohzawa, I., and Freeman, R.D. (1993a). Spatiotemporal organization of simple-cell receptive fields in the cat's striate cortex. I. General characteristics and postnatal development. J. Neurophysiol. *69*, 1091–1117.

DeAngelis, G.C., Ohzawa, I., and Freeman, R.D. (1993b). Spatiotemporal organization of simple-cell receptive fields in the cat's striate cortex. II. Linearity of temporal and spatial summation. J. Neurophysiol. *69*, 1118–1135.

DeAngelis, G.C., Freeman, R.D., and Ohzawa, I. (1994). Length and width tuning of neurons in the cat's primary visual cortex. J. Neurophysiol. *71*, 347–374.

Douglas, R.J., and Martin, K.A.C. (1991). A functional microcircuit for cat visual cortex. J. Physiol. *440*, 735–769.

Douglas, R.J., Martin, K.A.C., and Whitteridge, D. (1991). An intracellular analysis of the visual responses of neurones in cat visual cortex. J. Physiol. *440*, 659–696.

Eysel, U.T., Crook, J.M., and Machemer, H.F. (1990). GABA-induced remote inactivation reveals cross-orientation inhibition in the cat striate cortex. Exp. Brain Res. *80*, 626–630.

Ferster, D. (1981). A comparison of binocular depth mechanisms in areas 17 and 18 of the cat visual cortex. J. Physiol. *311*, 623–655.

Ferster, D. (1986). Orientation selectivity of synaptic potentials in neurons of cat primary visual cortex. J. Neurosci. *6*, 1284–1301.

Ferster, D. (1988). Spatially opponent excitation and inhibition in simple cells of the cat visual cortex. J. Neurosci. *8*, 1172–1180.

Ferster, D., and Lindström, S. (1983). An intracellular analysis of geniculocortical connectivity in area 17 of the cat. J. Physiol. *342*, 181–215.

Ferster, D., Chung, S., and Wheat, H. (1996). Orientation selectivity of thalamic input to simple cells of cat visual cortex. Nature *380*, 249–252.

Finn, I.M., Priebe, N.J., and Ferster, D. (2007). The emergence of contrast-invariant orientation tuning in simple cells of the cat visual cortex. Neuron *54*, 137–152.

Frazor, R.A., Albrecht, D.G., Geisler, W.S., and Crane, A.M. (2004). Visual cortex neurons of monkeys and cats: temporal dynamics of the spatial frequency response function. J. Neurophysiol. *91*, 2607–2627.

Freeman, T.C., Durand, S., Kiper, D.C., and Carandini, M. (2002). Suppression without inhibition in visual cortex. Neuron *35*, 759–771.

Fujita, I., and Konishi, M. (1991). The role of GABAergic inhibition in processing of interaural time difference in the owl's auditory system. J. Neurosci. *11*, 722–739.

Gardner, J.L., Anzai, A., Ohzawa, I., and Freeman, R.D. (1999). Linear and nonlinear contributions to orientation tuning of simple cells in the cat's striate cortex. Vis. Neurosci. *16*, 1115–1121.

Gillespie, D., Lampl, L., Anderson, J.S., and Ferster, D. (2001). Dynamics of the orientation tuned membrane potential response in cat primary visual cortex. Nat. Neurosci. *4*, 1014–1019.

Hansel, D., and Sompolinsky, H. (1996). Chaos and synchrony in a model of a hypercolumn in visual cortex. J. Comput. Neurosci. *3*, 7–34.

Hansel, D., and van Vreeswijk, C. (2002). How noise contributes to contrast invariance of orientation tuning in cat visual cortex. J. Neurosci. *22*, 5118–5128.

Hartline, H.K. (1949). Inhibition of activity of visual receptors by illuminating nearby retinal areas in the Limulus eye. Fed. Proc. *8*, 69.

Heeger, D.J. (1992). Normalization of cell responses in cat striate cortex. Vis. Neurosci. *9*, 181–197.

Heeger, D.J. (1993). Modeling simple-cell direction selectivity with normalized, half-squared, linear operators. J. Neurophysiol. *70*, 1885–1898.

Heggelund, P. (1986). Quantitative studies of enhancement and suppression zones in the receptive field of simple cells in cat striate cortex. J. Physiol. *373*, 293–331.

Higley, M.J., and Contreras, D. (2006). Balanced excitation and inhibition determine spike timing during frequency adaptation. J. Neurosci. *26*, 448–457.

Hirsch, J.A., and Martinez, L.M. (2006). Circuits that build visual cortical receptive fields. Trends Neurosci. *29*, 30–39.

Hirsch, J.A., Alonso, J.M., Reid, R.C., and Martinez, L.M. (1998). Synaptic integration in striate cortical simple cells. J. Neurosci. *18*, 9517–9528.

Hirsch, J.A., Martinez, L.M., Pillai, C., Alonso, J.M., Wang, Q., and Sommer, F.T. (2003). Functionally distinct inhibitory neurons at the first stage of visual cortical processing. Nat. Neurosci. *6*, 1300–1308.

Hubel, D.H., and Wiesel, T.N. (1962). Receptive fields, binocular interaction and functional architecture in the cat's visual cortex. J. Physiol. *160*, 106–154.

Hubel, D.H., and Wiesel, T.N. (1968). Receptive fields and functional architecture of monkey striate cortex. J. Physiol. *195*, 215–243.

Jagadeesh, B., Wheat, H.S., and Ferster, D. (1993). Linearity of summation of synaptic potentials underlying direction selectivity in simple cells of the cat visual cortex. Science *262*, 1901–1904.

Jin, J.Z., Weng, C., Yeh, C.I., Gordon, J.A., Ruthazer, E.S., Stryker, M.P., Swadlow, H.A., and Alonso, J.M. (2008). On and off domains of geniculate afferents in cat primary visual cortex. Nat. Neurosci. *11*, 88–94.

Jones, J.P., and Palmer, L.A. (1987). The two-dimensional spatial structure of simple receptive fields in cat striate cortex. J. Neurophysiol. *58*, 1187–1211.

Khawaled, R., Bruening-Wright, A., Adelman, J.P., and Maylie, J. (1999). Bicuculline block of small-conductance calcium-activated potassium channels. Eur. J. Phys. *438*, 314–321.

Kelly, M.K., Carvell, G.E., Kodger, J.M., and Simons, D.J. (1999). Sensory loss by selected whisker removal produces immediate disinhibition in the somatosensory cortex of behaving rats. J. Neurosci. *19*, 9117–9125.

Kuffler, S.W. (1953). Discharge patterns and functional organization of mammalian retina. J. Neurophysiol. *16*, 37–68.

Lampl, L., Anderson, J.S., Gillespie, D., and Ferster, D. (2001). Prediction of orientation selectivity from receptive field architecture in simple cells of cat visual cortex. Neuron *30*, 263–274.

Latham, P.E., and Nirenberg, S. (2004). Computing and stability in cortical networks. Neural Comput. *16*, 1385–1412.

Levitt, J.B., and Lund, J.S. (1997). Contrast dependence of contextual effects in primate visual cortex. Nature *387*, 73–76.

Li, C.Y., and Li, W. (1994). Extensive integration field beyond the classical receptive field of cat's striate cortical neurons–classification and tuning properties. Vision Res. *34*, 2337–2355.

Li, B., Thompson, J.K., Duong, T., Peterson, M.R., and Freeman, R.D. (2006). Origins of cross-orientation suppression in the visual cortex. J. Neurophysiol. *96*, 1755–1764.

Martinez, L.M., Alonso, J.M., Reid, R.C., and Hirsch, J.A. (2002). Laminar processing of stimulus orientation in cat visual cortex. J. Physiol. *540*, 321–333.

Martinez, L.M., Wang, Q., Reid, R.C., Pillai, C., Alonso, J.M., Sommer, F.T., and Hirsch, J.A. (2005). Receptive field structure varies with layer in the primary visual cortex. Nat. Neurosci. *8*, 372–379.

Mazer, J.A., Vinje, W.E., McDermott, J., Schiller, P.H., and Gallant, J.L. (2002). Spatial frequency and orientation tuning dynamics in area V1. Proc. Natl. Acad. Sci. USA *99*, 1645–1650.

McCormick, D.A., Connors, B.W., Lighthall, J.W., and Prince, D.A. (1985). Comparative electrophysiology of pyramidal and sparsely spiny stellate neurons of the neocortex. J. Neurophysiol. *54*, 782–806.

Mclean, J., and Palmer, L.A. (1988). Contribution of linear mechanisms to direction selectivity of simple cells in area 17 and 18 of the cat. Invest. Ophthalmol. Vis. Sci. *29* (*Suppl.*), 23.

Mechler, F., and Ringach, D.L. (2002). On the classification of simple and complex cells. Vision Res. *42*, 1017–1033.

Miller, K.D., and Troyer, T.W. (2002). Neural noise can explain expansive, power-law nonlinearities in neural response functions. J. Neurophysiol. *87*, 653–659.

Mirman, D., McClelland, J.L., and Holt, L.L. (2005). Computational and behavioral investigations of lexically induced delays in phoneme recognition. J. Mem. Lang. *52*, 424–433.

Moore, C.I., and Nelson, S.B. (1998). Spatio-temporal subthreshold receptive fields in the vibrissa representation of rat primary somatosensory cortex. J. Neurophysiol. *80*, 2882–2892.

Mooser, F., Bosking, W.H., and Fitzpatrick, D. (2004). A morphological basis for orientation tuning in primary visual cortex. Nat. Neurosci. *7*, 872–879.

Morrone, M.C., Burr, D.C., and Speed, H.D. (1987). Cross-orientation inhibition in cat is GABA mediated. Exp. Brain Res. *67*, 635–644.

Movshon, J.A., Thompson, I.D., and Tolhurst, D.J. (1978). Spatial and temporal contrast sensitivity of neurones in areas 17 and 18 of the cat's visual cortex. J. Physiol. *283*, 101–120.

Nelson, S., Toth, L., Sheth, B., and Sur, M. (1994). Orientation selectivity of cortical neurons during intracellular blockade of inhibition. Science *265*, 774–777.

Nowak, L.G., Sanchez-Vives, M.V., and McCormick, D.A. (2007). Lack of orientation and direction selectivity in a subgroup of fast-spiking inhibitory interneurons: Cellular and synaptic mechanisms and comparison with other electrophysiological cell types. Cereb. Cortex, in press. 10.1093/cercor/bhm137.

Olsen, J.F., and Suga, N. (1991). Combination-sensitive neurons in the medial geniculate body of the mustached bat: encoding of relative velocity information. J. Neurophysiol. *65*, 1254–1274.

Ozeki, H., Sadakane, O., Akasaki, T., Naito, T., Shimegi, S., and Sato, H. (2004). Relationship between excitation and inhibition underlying size tuning and contextual response modulation in the cat primary visual cortex. J. Neurosci. *24*, 1428–1438.

Palmer, L.A., and Davis, T.L. (1981). Receptive-field structure in cat striate cortex. J. Neurophysiol. *46*, 260–276.

Park, T.J., Monsivais, P., and Pollak, G.D. (1997). Processing of interaural intensity differences in the LSO: role of interaural threshold differences. J. Neurophysiol. *77*, 2863–2878.

Priebe, N.J., and Ferster, D. (2005). Direction selectivity of excitation and inhibition in simple cells of the cat primary visual cortex. Neuron *45*, 133–145.

Priebe, N.J., and Ferster, D. (2006). Mechanisms underlying cross-orientation suppression in cat visual cortex. Nat. Neurosci. *9*, 552–561.

Priebe, N.J., Mechler, F., Carandini, M., and Ferster, D. (2004). The contribution of spike threshold to the dichotomy of cortical simple and complex cells. Nat. Neurosci. *7*, 1113–1122.

Reid, R.C., and Alonso, J.M. (1995). Specificity of monosynaptic connections from thalamus to visual cortex. Nature *378*, 281–284.

Reid, R.C., Soodak, R.E., and Shapley, R.M. (1987). Linear mechanisms of directional selectivity in simple cells of cat striate cortex. Proc. Natl. Acad. Sci. USA *84*, 8740–8744.

Reid, R.C., Soodak, R.E., and Shapley, R.M. (1991). Directional selectivity and spatiotemporal structure of receptive fields of simple cells in cat striate cortex. J. Neurophysiol. *66*, 505–529.

Reig, R., Gallego, R., Nowak, L.G., and Sanchez-Vives, M.V. (2006). Impact of cortical network activity on short-term synaptic depression. Cereb. Cortex *16*, 688–695.

Ringach, D.L., and Malone, B.J. (2007). The operating point of the cortex: neurons as large deviation detectors. J. Neurosci. *27*, 7673–7683.

Ringach, D.L., Hawken, M.J., and Shapley, R. (1997). Dynamics of orientation tuning in macaque primary visual cortex. Nature *387*, 281–284.

Ringach, D.L., Hawken, M.J., and Shapley, R. (2003). Dynamics of orientation tuning in macaque V1: the role of global and tuned suppression. J. Neurophysiol. *90*, 342–352.

Ringach, D.L., Shapley, R.M., and Hawken, M.J. (2002). Orientation selectivity in macaque V1: diversity and laminar dependence. J. Neurosci. *22*, 5639–5651.

Rose, D., and Blakemore, C. (1974). Effects of bicuculline on functions of inhibition in visual cortex. Nature *249*, 375–377.

Rust, N.C., Schwartz, O., Movshon, J.A., and Simoncelli, E.P. (2005). Spatiotemporal elements of macaque v1 receptive fields. Neuron *46*, 945–956.

Saul, A.B., and Humphrey, A.L. (1992). Evidence of input from lagged cells in the lateral geniculate nucleus to simple cells in cortical area 17 of the cat. J. Neurophysiol. *68*, 1190–1208.

Sclar, G., and Freeman, R.D. (1982). Orientation selectivity in the cat's striate cortex is invariant with stimulus contrast. Exp. Brain Res. *46*, 457–461.

Shadlen, M.N., and Newsome, W.T. (1998). The variable discharge of cortical neurons: implications for connectivity, computation, and information coding. J. Neurosci. *18*, 3870–3896.

Sillito, A.M. (1975). The contribution of inhibitory mechanisms to the receptive field properties of neurones in the striate cortex of the cat. J. Physiol. *250*, 305–329.

Sillito, A.M., and Jones, H.E. (2002). Corticothalamic interactions in the transfer of visual information. Philos. Trans. R Soc. Lond. B Biol. Sci. *357*, 1739–1752.

Sillito, A.M., Kemp, J.A., Milson, J.A., and Berardi, N. (1980). A re-evaluation of the mechanisms underlying simple cell orientation selectivity. Brain Res. *194*, 517–520.

Sillito, A.M., Cudeiro, J., and Murphy, P.C. (1993). Orientation sensitive elements in the corticofugal influence on centre-surround interactions in the dorsal lateral geniculate nucleus. Exp. Brain Res. *93*, 6–16.

Skottun, B.C., Bradley, A., Sclar, G., Ohzawa, I., and Freeman, R. (1987). The effects of contrast on visual orientation and spatial frequency discrimination: a comparison of single cells and behavior. J. Neurophysiol. *57*, 773–786.

Skottun, B.C., De Valois, R.L., Grosof, D.H., Movshon, J.A., Albrecht, D.G., and Bonds, A.B. (1991). Classifying simple and complex cells on the basis of response modulation. Vision Res. *31*, 1079–1086.

Smith, M.A., Bair, W., and Movshon, J.A. (2006). Dynamics of suppression in macaque primary visual cortex. J. Neurosci. *26*, 4826–4834.

Somers, D.C., Nelson, S.B., and Sur, M. (1995). An emergent model of orientation selectivity in cat visual cortical simple cells. J. Neurosci. *15*, 5448–5465.

Sompolinsky, H., and Shapley, R. (1997). New perspectives on the mechanisms for orientation selectivity. Curr. Opin. Neurobiol. *7*, 514–522.

Sompolinsky, H., Golomb, D., and Kleinfeld, D. (1990). Global processing of visual stimuli in a neural network of coupled oscillators. Proc. Natl. Acad. Sci. USA *87*, 7200–7204.

Suga, N., Zhang, Y., and Yan, J. (1997). Sharpening of frequency tuning by inhibition in the thalamic auditory nucleus of the mustached bat. J. Neurophysiol. *77*, 2098–2114.

Swadlow, H.A. (2002). Thalamocortical control of feed-forward inhibition in awake somatosensory 'barrel' cortex. Philos. Trans. R. Soc. Lond. B Biol. Sci. *357*, 1717–1727.

Swadlow, H.A. (2003). Fast-spike interneurons and feedforward inhibition in awake sensory neocortex. Cereb. Cortex *13*, 25–32.

Swadlow, H.A., Beloozerova, I.N., and Sirota, M.G. (1998). Sharp, local synchrony among putative feed-forward inhibitory interneurons of rabbit somatosensory cortex. J. Neurophysiol. *79*, 567–582.

Tan, A.Y., Zhang, L.I., Merzenich, M.M., and Schreiner, C.E. (2004). Tone-evoked excitatory and inhibitory synaptic conductances of primary auditory cortex neurons. J. Neurophysiol. *92*, 630–643.

Tanaka, K. (1983). Cross-correlation analysis of geniculostriate neuronal relationships in cats. J. Neurophysiol. *49*, 1303–1318.

Tolhurst, D.J., and Dean, A.F. (1991). Evaluation of a linear model of directional selectivity in simple cells of the cat's striate cortex. Vis. Neurosci. *6*, 421–428.

Tolhurst, D.J., and Heeger, D.J. (1997). Comparison of contrast-normalization and threshold models of the responses of simple cells in cat striate cortex. Vis. Neurosci. *14*, 293–309.

Torre, V., and Poggio, T. (1978). A synaptic mechanism possibly underlying direction selectivity to motion. Proc. R. Soc. Lond. B. Biol. Sci. *202*, 409–416.

Troyer, T.W., Krukowski, A.E., and Miller, K.D. (2002). LGN input to simple cells and contrast-invariant orientation tuning: an analysis. J. Neurophysiol. *87*, 2741–2752.

Tsodyks, M.V., and Markram, H. (1997). The neural code between neocortical pyramidal neurons depends on neurotransmitter release probability. Proc. Natl. Acad. Sci. USA *94*, 719–723.

Tsodyks, M.V., Skaggs, W.E., Sejnowski, T.J., and McNaughton, B.L. (1997). Paradoxical effects of external modulation of inhibitory interneurons. J. Neurosci. *17*, 4382–4388.

van Vreeswijk, C., and Sompolinsky, H. (1998). Chaotic balanced state in a model of cortical circuits. Neural Comput. *10*, 1321–1371.

Vandenbeuch, A., Pillias, A.M., and Faurion, A. (2004). Modulation of taste peripheral signal through interpapillar inhibition in hamsters. Neurosci. Lett. *358*, 137–141.

Volgushev, M., Pernberg, J., and Eysel, U.T. (2000). Comparison of the selectivity of postsynaptic potentials and spike responses in cat visual cortex. Eur. J. Neurosci. *12*, 257–263.

Walker, G.A., Ohzawa, I., and Freeman, R.D. (1998). Binocular cross-orientation suppression in the cat's striate cortex. J. Neurophysiol. *79*, 227–239.

Wang, J., Caspary, D., and Salvi, R.J. (2000). GABA-A antagonist causes dramatic expansion of tuning in primary auditory cortex. Neuroreport *11*, 1137–1140.

Wang, J., McFadden, S.L., Caspary, D., and Salvi, R. (2002). Gamma-aminobutyric acid circuits shape response properties of auditory cortex neurons. Brain Res. *944*, 219–231.

Watson, A.B., and Ahumada, A.J. (1983). A look at motion in the frequency domain. In Motion: Perception and representation, J.K. Tsotsos, ed. (New York: Association for Computing Machinery), pp. 1–10.

Wehr, M., and Zador, A.M. (2003). Balanced inhibition underlies tuning and sharpens spike timing in auditory cortex. Nature *426*, 442–446.

Wilson, R.I., and Mainen, Z.F. (2006). Early events in olfactory processing. Annu. Rev. Neurosci. *29*, 163–201.

Worgotter, F., and Eysel, U.T. (1991). Topographical aspects of intracortical excitation and enhibition contributing to orientation specificity in area 17 of the cat visual cortex. Eur. J. Neurosci. *3*, 1232–1244.

Xie, R., Meitzen, J., and Pollak, G.D. (2005). Differing roles of inhibition in hierarchical processing of species-specific calls in auditory brainstem nuclei. J. Neurophysiol. *94*, 4019–4037.

Xing, D., Shapley, R.M., Hawken, M.J., and Ringach, D.L. (2005). Effect of stimulus size on the dynamics of orientation selectivity in Macaque V1. J. Neurophysiol. *94*, 799–812.

Yang, L., Pollak, G.D., and Resler, C. (1992). GABAergic circuits sharpen tuning curves and modify response properties in the mustache bat inferior colliculus. J. Neurophysiol. *68*, 1760–1774.

Zhang, L.I., Tan, A.Y., Schreiner, C.E., and Merzenich, M.M. (2003). Topography and synaptic shaping of direction selectivity in primary auditory cortex. Nature *424*, 201–205.

Zhu, J.J., and Connors, B.W. (1999). Intrinsic firing patterns and whisker-evoked synaptic responses of neurons in the rat barrel cortex. J. Neurophysiol. *81*, 1171–1183.